Nuclear Engineering and Technology 48 (2016) 1264–1272

Available online at ScienceDirect

Nuclear Engineering and Technology

journal homepage: www.elsevier.com/locate/net

Original Article

Estimation of Leak Rate Through Cracks in Bimaterial Pipes in Nuclear Power Plants

Jai Hak Park [a,*], *Jin Ho Lee* [b], *and Young-Jin Oh* [c]

[a] *Department of Safety Engineering, Chungbuk National University, 1 Chungdae-ro, Seowon-gu, Cheongju, Chungbuk 362-763, South Korea*

[b] *Department of Mechanical and Material Assessment, Korea Institute of Nuclear Safety, 62 Gwahak-ro, Yuseong-gu, Daejeon 305-338, South Korea*

[c] *Department of Structural Integrity and Materials, KEPCO Engineering and Construction Company, 269 Hyeoksin-ro, Gimcheon, Kyeongbuk 740-220, South Korea*

ARTICLE INFO

Article history:
Received 30 September 2015
Received in revised form
15 April 2016
Accepted 2 May 2016
Available online 31 May 2016

Keywords:
Crack
Crack Morphology Parameter
Flow Model
Henry–Fauske Flow Model
Leak Rate
Nuclear Power Plant
Pipe

ABSTRACT

The accurate estimation of leak rate through cracks is crucial in applying the leak before break (LBB) concept to pipeline design in nuclear power plants. Because of its importance, several programs were developed based on the several proposed flow models, and used in nuclear power industries. As the flow models were developed for a homogeneous pipe material, however, some difficulties were encountered in estimating leak rates for bimaterial pipes. In this paper, a flow model is proposed to estimate leak rate in bimaterial pipes based on the modified Henry–Fauske flow model. In the new flow model, different crack morphology parameters can be considered in two parts of a flow path. In addition, based on the proposed flow model, a program was developed to estimate leak rate for a crack with linearly varying cross-sectional area. Using the program, leak rates were calculated for through-thickness cracks with constant or linearly varying cross-sectional areas in a bimaterial pipe. The leak rate results were then compared and discussed in comparison with the results for a homogeneous pipe. The effects of the crack morphology parameters and the variation in cross-sectional area on the leak rate were examined and discussed.

1. Introduction

The accurate estimation of leak rate through cracks is crucial in applying the *leak before break* (LBB) concept to pipeline design in nuclear power plants. Because of its importance, many flow models were proposed and used in several programs, such as PICEP [1,2], SQUIRT [3], and PRAISE [4,5]. In the SQUIRT and PRAISE programs, the Henry–Fauske flow model [6–8] was used. In this model, nonequilibrium vapor generation rates were considered and also the pressure loss terms due to friction, bends, and protrusions in the crack flow path were included in the governing equations.

Rahman et al [9] introduced a new flow model after modifying the Henry–Fauske flow model. In the previous

* *Corresponding author.*
E-mail address: jhpark@chungbuk.ac.kr (J.H. Park).

http://dx.doi.org/10.1016/j.net.2016.05.005

model, the crack morphology parameters were assumed to be constant along the flow path. In the new model, however, the crack morphology parameters are assumed to be a function of crack opening displacement (COD). This modified Henry–Fauske model was implemented in the PRO-LOCA program [10], which is a probabilistic fracture mechanics program for pipes, and also in the program developed by Park et al. [11].

In the previous flow models, only pipes made of a single material were considered. Therefore, it was difficult to estimate the flow rate through cracks in bimaterial pipes using the developed program. In this paper, the modified Henry–Fauske flow model was extended further to consider different crack morphology parameters in two parts of a flow path in a bimaterial pipe. In addition, a program was developed based on the proposed flow model. The proposed model can be used to estimate the leak rate of steam–water mixture through cracks in pipes or vessels. Using the program, the leak rate was calculated for through-thickness cracks with a constant or linearly varying cross-sectional area in a bimaterial pipe. In addition, the results were compared with the results for a homogeneous pipe. The default crack morphology parameters of corrosion fatigue and intergranular stress corrosion cracking (IGSCC) in the PRO-COCA program [10] were used in the calculation. The effects of the crack morphology parameters and the variation of cross-sectional area along a flow path on the leak rate were examined and discussed.

2. Materials and methods

2.1. Flow model for bimaterial pipes

To estimate leak rates for through-thickness cracks in bimaterial pipes, a new flow model was proposed by modifying the Henry–Fauske flow model, which was developed to estimate the leak rate of steam–water mixture in pipes and vessels in nuclear power plants. The flow path considered in the proposed model is illustrated in Fig. 1. The flow path in each material can have different crack morphology parameters and also can have a linearly varying cross-sectional area. Let the cross-sectional areas at the entrance, interface, and exit planes be A_o, A_m, and A_c,respectively, and let the pressures at each plane be p_o, p_m, and p_c.

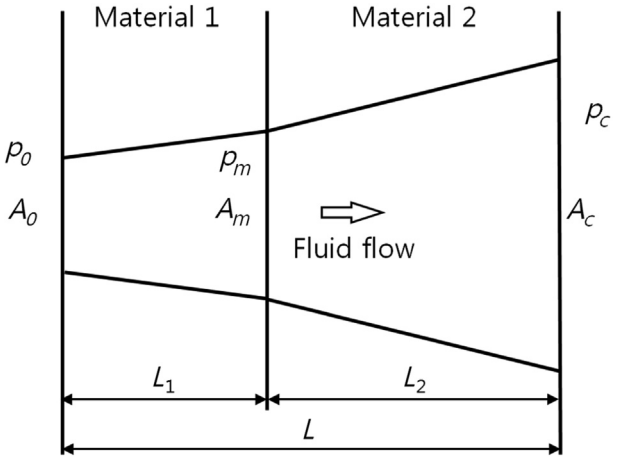

Fig. 1 – Flow path in a bimaterial pipe.

The Henry–Fauske flow model can be described using the following equations [3,6–8]:

$$G_c^2 - \frac{1}{\left[\frac{X_c v_{gc}}{\gamma_o p_c} - (v_{gc} - v_{Lc}) N_c \left(\frac{dX_E}{dp}\right)_c\right]} = 0 \tag{1}$$

$$p_c + p_e + p_a + p_f + p_k + p_{aa} - p_o = 0 \tag{2}$$

where G is mass flux, p is pressure, v_{gc} and v_{Lc} are specific volumes of saturated vapor and saturated liquid, respectively, and γ_o is the isentropic expansion coefficient. The subscripts o and c are the values at the crack entrance plane and at the crack exit plane, respectively. Therefore, p_o and p_c are the pressure values at the crack entrance and exit planes, respectively.

In Eq. (1), X_c is the nonequilibrium vapor generation rate and X_E is defined by $X_E = (S_o - S_{Lc})/(S_{gc} - S_{Lc})$ [6]. Here, S_o is the entropy at the crack entrance plane, S_{Lc} is the entropy of liquid at the crack exit plane, S_{gc} is the entropy of saturated vapor at the crack exit plane, N_c is N at the crack exit plane (N is defined by $N = 20X_E$ for $X_E < 0.05$ and $N = 1.0$ for $X_E \geq 0.05$) [6]. In Eq. (2), p_e, p_f, p_k, p_a, and p_{aa} are the pressure losses due to entrance effects, friction, bends and protrusions in the flow path, phase change acceleration, and area change acceleration, respectively.

In Eqs. (1) and (2), mass flux at crack exit plane, G_c, and pressure at the crack exit plane, p_c, are unknown variables. The leak rate through a crack can be estimated by multiplying G_c with the crack opening area at the crack exit plane, A_c. The pressure at the interface plane, p_m, is also an unknown variable and must be determined while solving the equations.

The detailed definition of each term in Eqs. (1) and (2) for homogeneous pipes can be found in elsewhere (see [6,11]). Each term needs to be modified for a flow path in a bimaterial pipe.

2.2. Pressure loss terms

The pressure loss due to entrance effects, p_e, is given by [3].

$$p_e = \frac{G_o^2 v_{Lo}}{2C_D^2} \tag{3}$$

where C_D is the coefficient of discharge and $C_D = 0.95$ is used in this study.

The pressure losses due to friction in the flow paths in Materials 1 and 2, p_{f1} and p_{f2}, respectively, are given by

$$p_{f1} = \left(f_1 \frac{L_1}{D_H}\right) \frac{\overline{G}_1^2}{2} \left[(1 - \overline{X})\overline{v}_L + \overline{X}\overline{v}_g\right]_1 \tag{4}$$

$$p_{f2} = \left(f_2 \frac{L_2}{D_H}\right) \frac{\overline{G}_2^2}{2} \left[(1 - \overline{X})\overline{v}_L + \overline{X}\overline{v}_g\right]_2 \tag{5}$$

where f_1 and f_2 are the friction factors in the flow paths in Materials 1 and 2, respectively, and L_1 and L_2 are the lengths of the flow paths in Materials 1 and 2, respectively; X is the fluid quality, and a bar on the variable means the average value in

the region. The subscripts 1 and 2 mean the values in the flow paths in Materials 1 and 2, respectively. Therefore, $\overline{G}_1$ and $\overline{G}_2$ refer to the mean values of the mass flux over the flow paths in Materials 1 and 2, respectively. $\overline{G}_1$ and $\overline{G}_2$ can be obtained from the following equations:

$$\overline{G}_1 = \frac{A_o G_o + A_m G_m}{A_o + A_m} \tag{6}$$

$$\overline{G}_2 = \frac{A_m G_m + A_c G_c}{A_m + A_c} \tag{7}$$

where D_H is the hydraulic diameter defined by $D_H = (4 \times \text{area})/(\text{wetted perimeter})$. Here, *area* is the cross-sectional area of the flow path. If the shape of cross section of the flow path is a crack with length2a, then $D_H = \text{area}/a$. The average D_H value for the whole flow path is given by

$$D_H = (D_{H1}L_1 + D_{H2}L_2)/L \tag{8}$$

where $D_{H1} = (A_o + A_m)/(a_o + a_m)$ and $D_{H2} = (A_m + A_c)/(a_m + a_c)$ and a_o, a_m, and a_c are the half crack lengths at the crack entrance, interface, and exit planes, respectively.

In the Henry–Fauske flow model, the flow path can be divided into two ranges of $x/D_H > 12$ and $0 < x/D_H < 12$. Here x is the distance along the flow path. The range $x/D_H > 12$ corresponds to the two-phase flow region with liquid and gas and the range $0 < x/D_H < 12$ corresponds to the single-phase flow region with only liquid [6]. Initially, Henry [6] used the condition $x/D_H = 12$ for saturated and subcooled liquid with a sharp inlet and constant sectional area. Later this condition was also used for flow paths with a linearly varying sectional area [4].

When the two-phase flow begins in the flow path in Material 1, p_{f1} can be expressed as follows:

$$p_{f1} = f_1\left(\frac{L_1}{D_H} - 12\right)\frac{\overline{G}_{1t}^2}{2}\left[(1-\overline{X})\overline{v}_L + \overline{X}\overline{v}_g\right]_{1t} + 12f_1\frac{\overline{G}_{1s}^2}{2}v_{Lo} \tag{9}$$

where the subscripts 1s and 1t mean the values in the single-phase flow region and the two-phase flow region in Material 1, respectively. When the two-phase flow begins in the flow path in Material 2, a similar equation can be derived without difficulty.

The friction factor f is given by

$$f = \left[C_1 \log\left(\frac{D_H}{\mu}\right) + C_2\right]^{-2} \tag{10}$$

where μ is the surface roughness and C_1 and C_2 are coefficients given by $C_1 = 3.39$, $C_2 = -0.866$ for $D_H/\mu \le 100$ and $C_1 = 2.0$, $C_2 = 1.14$ for $D_H/\mu > 100$ [3].

Rahman et al [9] expressed the surface roughness μ as a function of COD as follows:

$$\begin{array}{lll} \mu = \mu_L & \text{for} & 0 < \delta/\mu_G \le 0.1 \\ \mu = \mu_L + (\mu_G - \mu_L)(\delta/\mu_G - 0.1)/9.9 & \text{for} & 0.1 < \delta/\mu_G \le 10 \\ \mu = \mu_G & \text{for} & 10 < \delta/\mu_G \end{array} \tag{11}$$

where μ_L and μ_G are the local and global surface roughness values, respectively, and δ is COD at the crack center.

The pressure loss terms due to bends and protrusions in each flow path are given by

$$p_{k1} = (e_{v1})\frac{\overline{G}_1^2}{2}\left[(1-\overline{X})\overline{v}_L + \overline{X}\overline{v}_g\right]_1 \tag{12}$$

$$p_{k2} = (e_{v2})\frac{\overline{G}_2^2}{2}\left[(1-\overline{X})\overline{v}_L + \overline{X}\overline{v}_g\right]_2 \tag{13}$$

where e_{v1} and e_{v2} are the total loss coefficients over each flow path. The variable e_{v1} and e_{v2} can be determined experimentally by defining

$$e_{v1} = n_{t1}L_1, \quad e_{v2} = n_{t2}L_2 \tag{14}$$

where n_{t1} and n_{t2} are the numbers of velocity heads lost per unit flow path length for a given type of crack, and also represent the number of 90° turns per unit length in each flow path. The parameter n_t is assumed to be a function of COD at the crack center and δ is given as follows [9]:

$$\begin{array}{lll} n_t = n_{tL} & \text{for} & 0 < \delta/\mu_G \le 0.1 \\ n_t = n_{tL} - n_{tL}(\delta/\mu_G - 0.1)/11 & \text{for} & 0.1 < \delta/\mu_G \le 10 \\ n_t = 0.1\ n_{tL} & \text{for} & 10 < \delta/\mu_G \end{array} \tag{15}$$

where n_{tL} is the local number of 90° turns per unit flow path length.

The pressure loss due to phase change acceleration, p_a, is given by [3].

$$P_a = \overline{G}_T^2\left[(1-X_c)v_{Lc} + X_c v_{gc} - v_{Lc}\right] \tag{16}$$

where $\overline{G}_T$ is the mean value of mass flux in the two-phase region of the flow path. When the two-phase flow begins in the flow path in Material 1, P_a terms in each flow path are expressed as follows:

$$P_{a1} = \overline{G}_T^2\left[(1-X_m)v_{Lm} + X_m v_{gm} - v_{Lm}\right] \tag{17}$$

$$P_{a2} = \overline{G}_T^2\left\{\left[(1-X_c)v_{Lc} + X_c v_{gc} - v_{Lc}\right] - \left[(1-X_m)v_{Lm} + X_m v_{gm} - v_{Lm}\right]\right\} \tag{18}$$

When the two-phase flow begins at $x = L_i$ in Material 1, x is the distance along flow path. Then we can get $L_i/D_H = 12$. The cross-sectional area at $x = L_i$, A_i can be obtained using the relation, $A_i = A_o + 12(A_m - A_o)D_H/L_1$. Then the mean cross-sectional area in the two-phase region of the flow path A_t is expressed as follows:

$$A_t = \frac{(A_i + A_m)(L_1 - 12D_H) + (A_m + A_c)L_2}{2(L - 12D_H)} \tag{19}$$

Then $\overline{G}_T$ has a relationship with G_c as $\overline{G}_T = (A_c/A_t)G_c$. When the two-phase flow begins in the flow path in Material 2, P_a terms in each material are expressed as follows:

$$P_{a1} = 0 \tag{20}$$

$$P_{a2} = \overline{G}_T^2\left[(1-X_c)v_{Lc} + X_c v_{gc} - v_{Lc}\right] \tag{21}$$

The cross-sectional area at $x = L_i$, A_i can be obtained using the relation $A_i = A_m + (A_c - A_m)(12D_H - L_1)/L_2$. Then the mean cross-sectional area in the two-phase region of the flow path A_t is expressed as $A_t = (A_i + A_c)/2$.

Next the pressure loss due to area change acceleration p_{aa} is considered. When the two-phase flow begins in Material 1, p_{aa} terms in each flow path can be expressed as follows:

$$p_{aa1} = \frac{G_m^2 v_{Lo}}{2}\left[\left(\frac{A_m}{A_i}\right)^2 - \left(\frac{A_m}{A_o}\right)^2\right] + \frac{G_m^2}{2}\left[(1-X)v_L + Xv_g\right]_1 \times \left[1 - \left(\frac{A_m}{A_i}\right)^2\right] \quad (22)$$

$$p_{aa2} = \frac{G_c^2}{2}\left[(1-X)v_L + Xv_g\right]_2\left[1 - \left(\frac{A_c}{A_m}\right)^2\right] \quad (23)$$

When the two-phase flow begins in Material 2, p_{aa} terms in each material can be expressed as follows:

$$p_{aa1} = \frac{G_m^2 v_{Lo}}{2}\left[1 - \left(\frac{A_m}{A_o}\right)^2\right] \quad (24)$$

$$p_{aa2} = \frac{G_c^2 v_{Lo}}{2}\left[\left(\frac{A_c}{A_i}\right)^2 - \left(\frac{A_c}{A_m}\right)^2\right] + \frac{G_c^2}{2}\left[(1-X)v_L + Xv_g\right]_2 \times \left[1 - \left(\frac{A_c}{A_i}\right)^2\right] \quad (25)$$

Because the flow path is not perpendicular to the pipe surface and not straight, the real flow path length is longer than the wall thickness. The real path length, L_a, can be obtained by multiplying the wall thickness, t with a flow path deviation factor K as follows:

$$L_a = Kt \quad (26)$$

The factor K is also given as a function of δ as follows [9]:

$$\begin{aligned} K &= K_{GL} && \text{for} \quad 0 < \delta/\mu_G \le 0.1 \\ K &= K_{GL} - (K_{GL} - K_G)(\delta/\mu_G - 0.1)/9.9 && \text{for} \quad 0.1 < \delta/\mu_G \le 10 \\ K &= K_G && \text{for} \quad 10 < \delta/\mu_G \end{aligned} \quad (27)$$

where K_G is the global path deviation factor and K_{GL} is the local waviness path deviation factor.

2.3. Solution of equations

Considering the relation $G_oA_o = G_mA_m = G_cA_c$ and examining the final expressions for the pressure loss terms, it can be noticed that the pressure loss terms p_e, p_f, p_k, p_a, and p_{aa} can be expressed as a function of G_c. Therefore, from Eq. (2), p_c can be expressed as a function of G_c. Substituting this relationship into Eq. (1), an equation, which contains the unknown variable G_c only, can be obtained.

As mentioned earlier, the pressure at the interface plane p_m is also an unknown variable. In the program, p_m is determined using iteration procedure as follows:

1. Assume an initial value for p_m.
2. Obtain p_c and G_c using Eqs. (1) and (2).
3. Calculate pressure loss terms p_e, p_{f1}, p_{k1} p_{a1}, and p_{aa1} for the flow path in Material 1.
4. Calculate updated p_m using the relationship $p_m = p_o - p_e - p_{f1} - p_{k1} - p_{a1} - p_{aa1}$.
5. Iterate the steps from (2) to (4) until converged p_m is obtained.

Table 1 – Mean and standard deviation of crack morphology parameters [10].

Crack morphology variable	Corrosion fatigue		Intergranular stress corrosion cracking	
	Mean	SD	Mean	SD
μ_L (μm)	8.814	2.972	4.70	3.937
μ_G (μm)	40.51	17.65	80.0	39.01
n_L (1/mm)	6.730	8.070	28.2	18.90
K_G	1.017	0.0163	1.07	0.100
K_{GL}	1.060	0.0300	1.33	0.170

SD, standard deviation.

To calculate the pressure loss terms, the water and vapor properties must be calculated. The properties were calculated at the mean pressure in each flow path. The mean pressure values for the flow paths in Materials 1 and 2 were assumed to be $(p_o + p_m)/2$ and $(p_m + p_c)/2$ respectively.

3. Results and discussion

3.1. Comparison of the two flow models

A program was developed to estimate leak rate through a crack in a pipe using the proposed flow model for bimaterial pipes. Using the program, several problems were solved and examined.

First, leak rates were obtained for through-thickness cracks with the crack length $2a$ in homogeneous pipes. The cross-sectional area was assumed to be constant along the flow path. The crack morphology parameters and the values for corrosion fatigue are presented in Table 1. Leak rates were obtained using the two flow models (i.e., the previous model for homogeneous pipes and the new proposed model for bimaterial pipes). Even if the cross-sectional area and crack morphology parameters are constant along the flow path, the

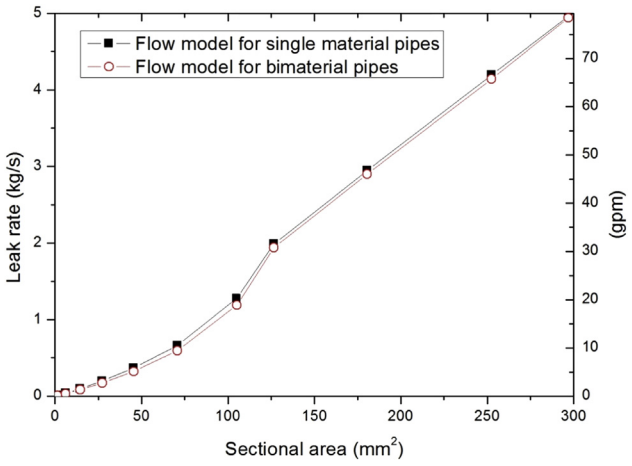

Fig. 2 – Comparison between leak rates obtained from the previous flow model for single material pipes and the flow model for bimaterial pipes.

Table 2 – Comparison of leak rates obtained from the two flow models.

Sectional area (mm^2)	Half crack length (mm)	Crack opening displacement (mm)	L/D_H	Leak rate from single material model (kg/s)	Leak rate from bimaterial model (kg/s)	Difference (%)
6.16	50.8	0.0745	586	0.0368	0.0313	−14.9
27.2	101.5	0.1642	265	0.1974	0.1713	−13.2
70.8	152.3	0.283	153.0	0.662	0.593	−10.5
105.1	177.6	0.359	120.1	1.276	1.187	−6.98
126.6	190.3	0.403	106.9	1.987	1.939	−2.41
180.5	216	0.506	85.0	2.95	2.90	−1.652
252	241	0.631	67.9	4.20	4.14	−1.284
297	254	0.704	60.8	4.97	4.94	−0.523

two flow models may give different leak rates because the definitions of several variables are different in each flow model.

In all problems considered in this study, the total thickness of pipe is 71.12 mm, and the operating pressure and temperature are 15.51 MPa and 288°C, respectively. In the proposed model, it was assumed that $L_1 = L_2$ in Fig. 1.

Fig. 2 shows the leak rate results. The solid symbols show the flow rates obtained from the previous flow model and the open holes from the proposed flow model. The detailed leak rates are also given in Table 2 including the half crack length, COD, and L/D_H values used in the calculation. It can be noted that in the small leak rate region, the proposed flow model gives about 15% less leak rate when compared with the previous flow model. However, the difference between the two models decreases as the leak rate increases.

Fig. 3 shows the normalized pressure loss terms obtained from the two flow models. In the figure, p_t/p_o is the normalized total pressure loss. The p_e/p_o terms were not included in the figure because they were very small compared with other pressure loss terms. It can be noted that the proposed flow model gives similar pressure loss terms to the previous model.

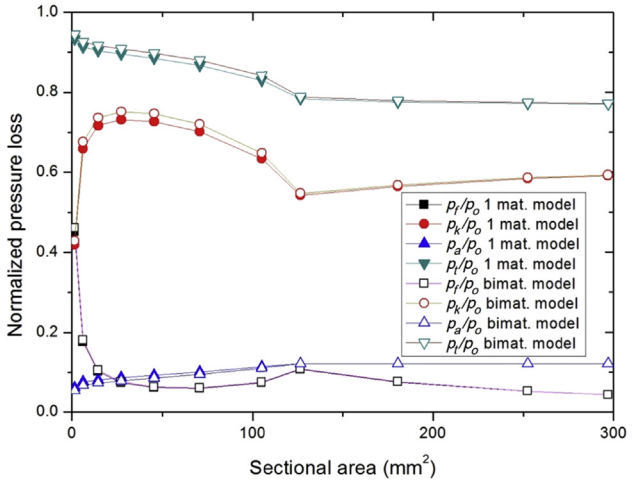

Fig. 3 – Comparison between normalized pressure loss terms obtained from the previous flow model for single material pipes and the flow model for bimaterial pipes. Here p_t is the total pressure loss. bi-mat., bimaterial.

3.2. *Effect of crack morphology parameter*

Next, the effect of crack morphology parameters on leak rate was examined. Leak rates were obtained for through-thickness cracks with a constant cross-sectional area. Four cases of crack morphology parameters were considered. In Case 1, crack morphology parameters were assumed to have the values of corrosion fatigue in Table 1 along the whole flow path. In Case 2, the values of IGSCC were assumed along the whole flow path. In Case 3, it was assumed that the first and the second halves of the flow path had the values of corrosion fatigue and IGSCC, respectively. In Case 4, the first and the second halves of the flow path had the values of IGSCC and corrosion fatigue, respectively.

The obtained leak rate results are shown in Fig. 4. As shown in the figure, Case 1 and Case 2 give the highest and the lowest leak rate, respectively, for a given cross-sectional area. Cases 3 and 4 give leak rates between those of Cases 1 and 2. The leak rates of Cases 3 and 4 show similar values, but the leak rate of Case 3 is a little higher than that of Case 4.

Several researchers have tried to estimate leak rates in bimaterial pipes using mean values of crack morphology

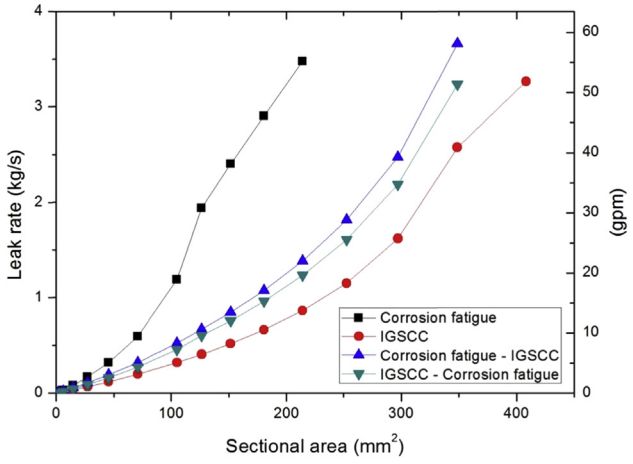

Fig. 4 – Effects of crack morphology parameters on the leak rates through cracks with constant cross-sectional areas. Four cases were considered: Case 1 (corrosion fatigue), Case 2 (IGSCC), Case 3 (corrosion fatigue – IGSCC), and Case 4 (IGSCC – corrosion fatigue). IGSCC, intergranular stress corrosion cracking.

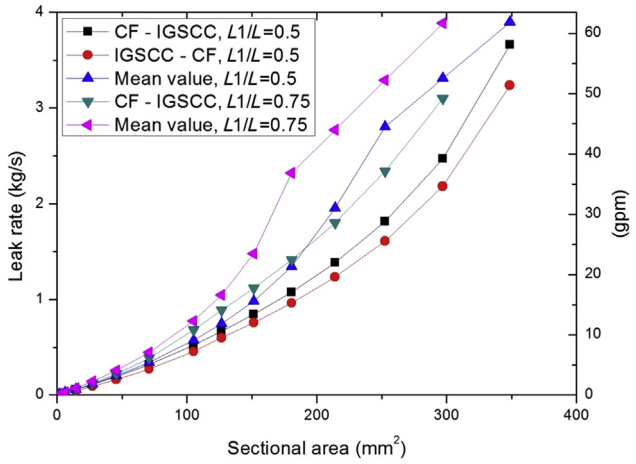

Fig. 5 – Comparison between the leak rates obtained from the flow mode for bimaterial pipes and from the previous flow model with mean crack morphology parameters. Here CF-IGSCC means that the crack morphology parameters of corrosion fatigue and IGSCC are used in the first and the second parts of the flow path and so forth. CF, corrosion fatigue; IGSCC, intergranular stress corrosion cracking.

parameters. Therefore, leak rates were obtained using the previous flow model with mean crack morphology parameters and compared with the leak rates obtained from the flow model for bimaterial pipes. For example, the mean value of μ_L along flow path is defined by

$$\overline{\mu}_L = (\mu_{L1}L_1 + \mu_{L2}L_2)/L \tag{28}$$

Fig. 5 shows the obtained leak rate results. The leak rates from the previous flow model with the mean crack morphology parameters were compared with the leak rates of Cases 3 and 4. In the region of the low leak rate, the two flow models show similar leak rates. As the leak rate increases, however, the previous flow model gives higher leak rates compared with the leak rates from the flow model for

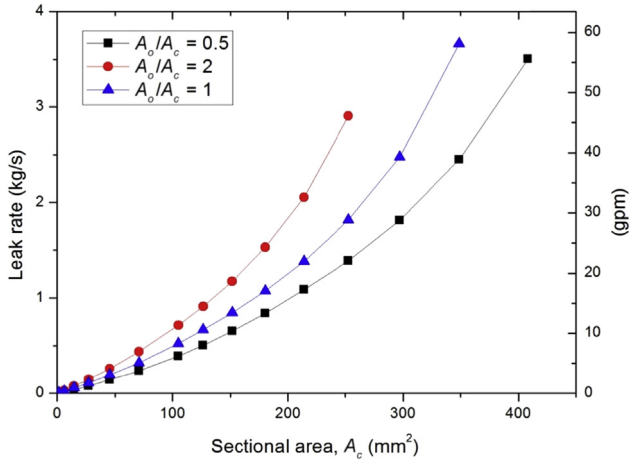

Fig. 6 – Effects of cross-sectional area at the entrance plane on the leak rates when the cross-sectional area varies linearly. The leak rates were plotted as a function of the cross-sectional area at the exit plane.

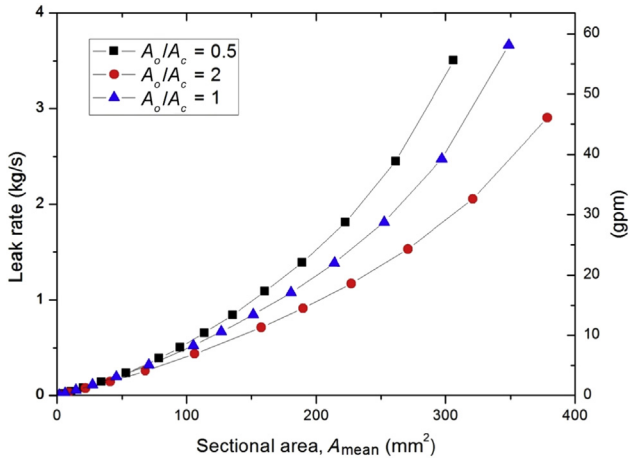

Fig. 7 – Effects of cross-sectional area at the entrance plane on the leak rates when the cross-sectional area varies linearly. The leak rates were plotted as a function of the mean cross-sectional area.

bimaterial pipes. The leak rates were also obtained when $L_1/L = 0.75$ and the first and the second parts of the flow path had the values of corrosion fatigue and IGSCC, respectively. It can also be noted that the previous flow model, with the mean crack morphology parameters, gives similar results only when the leak rate is low. As the leak rate increases, the estimated leak rate using the previous flow model is higher than the estimated value using the modified flow model for bimaterial pipes.

3.3. *Leak rates through a crack with linearly varying cross-sectional area*

Leak rates were calculated for through-thickness cracks with linearly varying cross-sectional areas. It was assumed that the first and second halves of the flow path had the crack morphology parameters of corrosion fatigue and IGSCC,

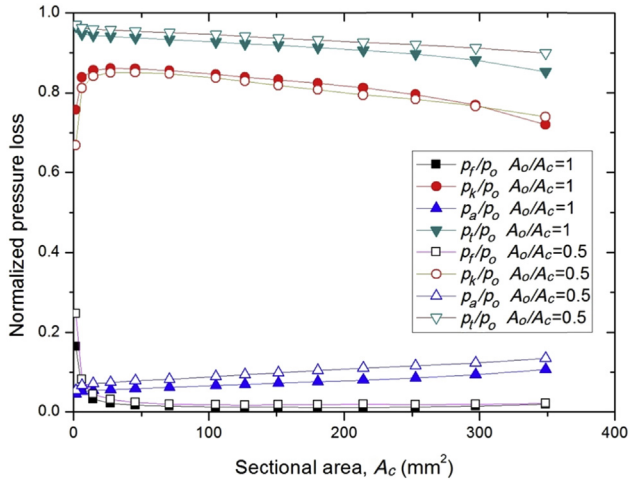

Fig. 8 – Comparison of normalized pressure loss terms obtained when $A_o/A_c = 1$ and $A_o/A_c = 0.5$. Here p_t is the total pressure loss.

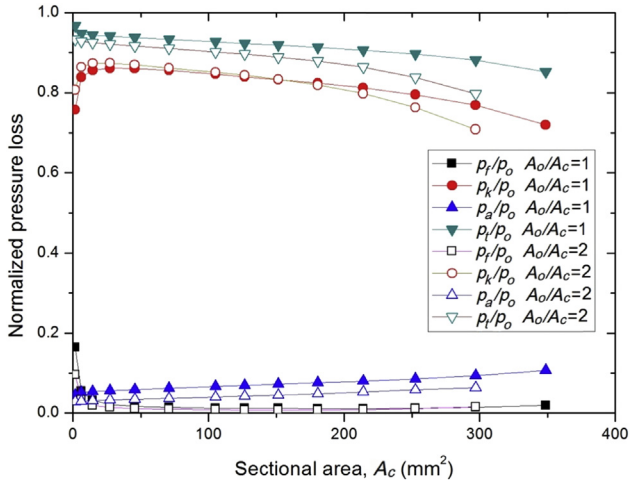

Fig. 9 – Comparison of normalized pressure loss terms obtained when $A_o/A_c = 1$ and $A_o/A_c = 2$. Here p_t is the total pressure loss.

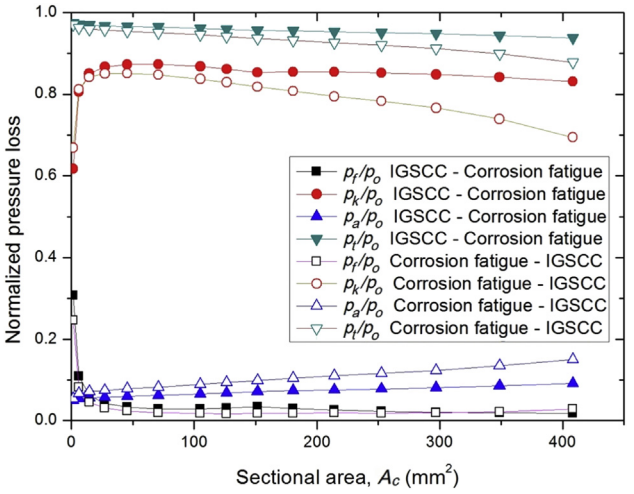

Fig. 11 – Comparison of normalized pressure loss terms between Case 3 (corrosion fatigue – IGSCC) and Case 4 (IGSCC – corrosion fatigue) when cross-sectional area varies linearly and $A_o/A_c = 0.5$. Here p_t is the total pressure loss. IGSCC, intergranular stress corrosion cracking.

respectively. The effect of the cross-sectional area at the entrance plane on leak rates was examined. The leak rates were obtained for the cases when A_o/A_c = 0.5, 1, and 2 and plotted as a function of cross-sectional area at the exit plane A_c as shown in Fig. 6. As expected, leak rate increases as A_o increases for a given A_c value. The leak rates were also plotted as a function of the mean cross-sectional area, A_{mean}, as shown in Fig. 7. Here A_{mean} is the mean of A_o and A_c. First, it was expected that the distance between the lines would be much decreased when the leak rates were plotted as a function of A_{mean}. However, the distance between the lines were not much decreased as shown in Fig. 7.

The normalized pressure loss terms were plotted in Fig. 8 when A_o/A_c = 1 and A_o/A_c = 0.5 The p_e/p_o and p_{aa}/p_o terms were not included in the figure because they were very small compared with other pressure loss terms. It can be noticed that the total pressure losses increase a little when A_o/A_c = 0.5, compared with the values when A_o/A_c = 1. The normalized pressure loss terms are also plotted in Fig. 9 when A_o/A_c = 1 and A_o/A_c = 2. In this case, the total pressure losses decrease when A_o/A_c = 2 compared with the values when A_o/A_c = 1.

The effect of crack morphology parameters on leak rate was examined for a flow path with a linearly varying cross-sectional area. Leak rates were obtained for a flow path with A_o/A_c = 0.5. Therefore, the cross-sectional area increases as fluid flows. As in the "Effect of Crack Morphology Parameter" section, four cases of crack morphology parameters were considered. In Cases 1 and 2, constant crack morphology parameters of corrosion fatigue and IGSCC were assumed, respectively. In Case 3, the first and second halves of the flow path were assumed to have the values of corrosion fatigue and

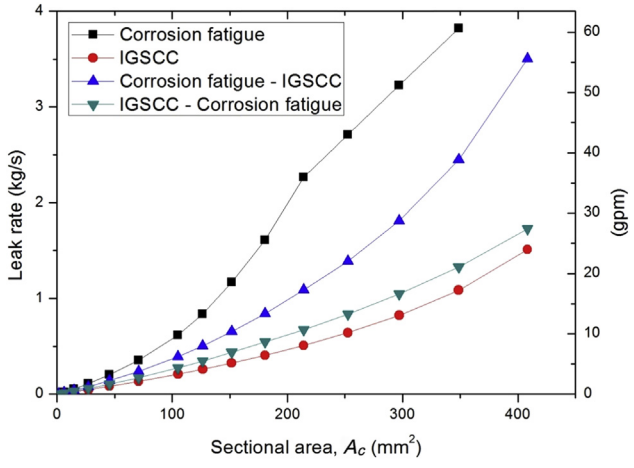

Fig. 10 – Effect of crack morphology parameters on the leak rate when cross-sectional area varies linearly and $A_o/A_c = 0.5$. IGSCC, intergranular stress corrosion cracking.

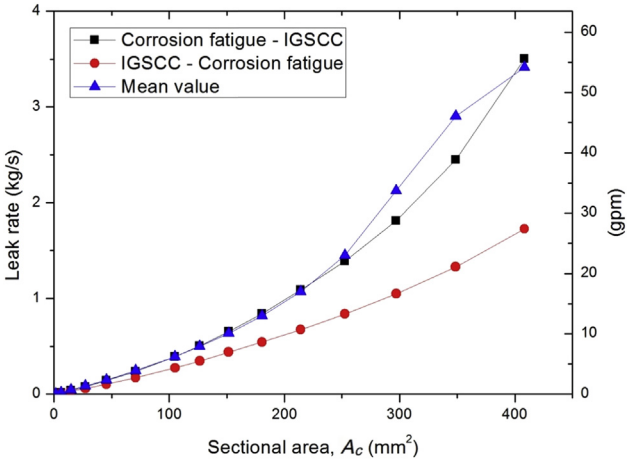

Fig. 12 – Comparison between the leak rates obtained from the flow model for bimaterial pipes and from the previous flow model with mean crack morphology parameters when $A_o/A_c = 0.5$. IGSCC, intergranular stress corrosion cracking.

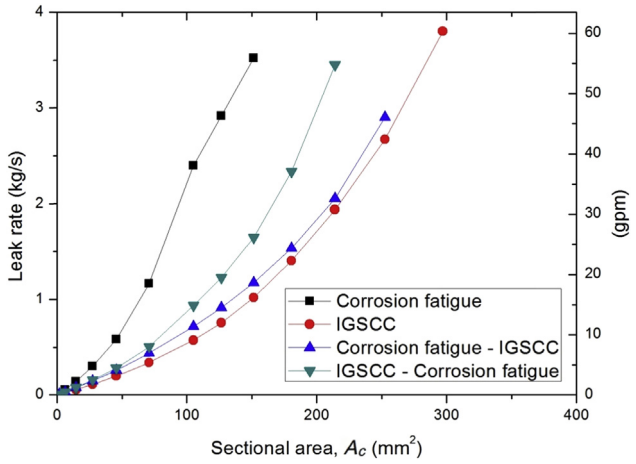

Fig. 13 – Effect of crack morphology parameters on the leak rate when the cross-sectional area varies linearly and $A_o/A_c = 2$. IGSCC, intergranular stress corrosion cracking.

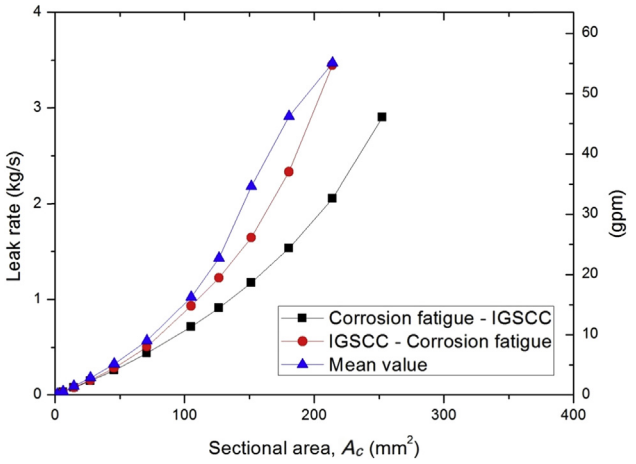

Fig. 15 – Comparison between the leak rates obtained from the flow model for bimaterial pipes and from the previous flow model with mean crack morphology parameters when $A_o/A_c = 2$. IGSCC, intergranular stress corrosion cracking.

IGSCC, respectively. In Case 4, the first and second halves had the values of IGSCC and corrosion fatigue, respectively.

Fig. 10 shows the leak rate results. As expected, Case 1 gives the highest and Case 2 gives the lowest leak rates. For the flow path with constant cross-sectional area, Cases 3 and 4 give similar leak rates as shown in Fig. 3, whereas for the flow path with linearly varying cross-sectional area, Case 3 gives a much higher leak rate than Case 4. From the results, it can be noted that the crack morphology parameters at the flow path with narrow cross-sectional area have more effect on the leak rate than the parameters at the flow path with larger cross-sectional area. The normalized pressure loss terms are plotted in Fig. 11 for Cases 3 and 4. It can be noted that the total pressure losses for Case 3 are less than those for Case 4.

Fig. 12 shows the leak rate obtained using the previous flow model with the mean crack morphology parameters. The leak rates were also compared with those of Cases 3 and 4. It can be noted that the previous flow model gives a similar leak rate to Case 3 and shows large discrepancy with Case 4.

The effect of crack morphology parameters was also examined for a flow path with a linearly varying cross-sectional area when $A_o/A_c = 2$. As shown in Fig. 13, Case 4 gives a much higher leak rate than Case 3. That is because the crack morphology parameters of the flow path with smaller cross-sectional area have a dominant effect. Fig. 14 shows the normalized pressure loss terms for Cases 3 and 4. It can be noted that the total pressure losses for Case 3 are larger than those for Case 4.

Fig. 15 shows the leak rate obtained from the previous flow model with the mean crack morphology parameters. The leak rates were also compared with those of Cases 3 and 4. The previous flow model gives a similar leak rate to Case 4.

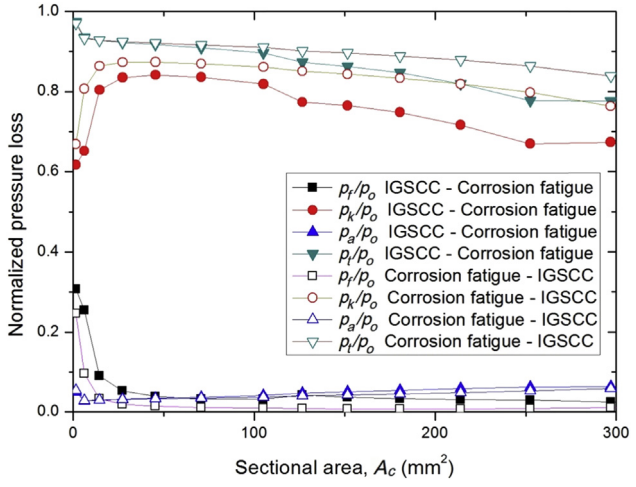

Fig. 14 – Comparison of normalized pressure loss terms between Case 3 (corrosion fatigue – IGSCC) and Case 4 (IGSCC – corrosion fatigue) when cross-sectional area varies linearly and $A_o/A_c = 2$. Here p_t is the total pressure loss. IGSCC, intergranular stress corrosion cracking.

4. Conclusion

1. A flow model was proposed to estimate leak rates for through-thickness cracks in bimaterial pipes in nuclear power plants based on the Henry–Fauske flow model.
2. The proposed flow model gives a similar leak rate to the previous flow model when a flow path has constant crack morphology parameters.
3. From the results of several sample problems it was recognized that the proposed flow model can be used effectively to estimate the leak rate in bimaterial pipes in nuclear power plants.
4. For a flow path with linearly varying cross-sectional area, the crack morphology parameters for the narrow region have a dominant effect on the leak rate.
5. When the previous flow model is used to estimate leak rates in bimaterial pipes with mean crack morphology parameters, caution should be exercised because the

previous flow model gives similar leak rates only when the cross-sectional area is constant and the leak rate is small, roughly less than 1 kg/s.

Conflicts of interest

All contributing authors declare no conflicts of interest.

Acknowledgments

This work was supported by the Nuclear Power Core Technology Development Program of the Korea Institute of Energy Technology Evaluation and Planning, with financial resources from the Ministry of Trade, Industry & Energy, Republic of Korea. (No. 20131520202170).

REFERENCES

[1] D.M. Norris, A. Okamoto, B. Chexal, T. Griesbach, PICEP: Pipe Crack Evaluation Program, EPRI Report Number EPRI NP-3596-SR, Electric Power Research Institute, Palo Alto, CA, 1984.
[2] H.S. Mehta, N.T. Patel, S. Ranganath, Application of the Leak-before-break Approach to BWR Piping, EPRI Report Number NP-4991, Electric Power Research Institute, Palo Alto, CA, 1986.
[3] D.D. Paul, J. Ahmad, P.M. Scott, L.E. Flanigan, G.M. Wilkowski, Evaluation and Refinement of Leak-rate Estimation Models, NUREG/CR-5128, Rev. 1, Battelle, Columbus (OH), 1994.
[4] D.O. Harris, D.D. Dedhia, S.C. Lu, Theoretical and User's Manual for Pc-PRAISE, USNRC Report NUREG/CR-5864, U.S. Nuclear Regulatory Commission, Washington, DC, 1992.
[5] D.O. Harris, D. Dedhia, WinPRAISE 07; Expanded PRAISE Code in Windows, Structural Integrity Associates, Inc., San Jose, CA, 2007.
[6] R.E. Henry, The two-phase critical discharge of initially saturated or subcooled liquid, Nucl. Sci. Eng. 41 (1970) 336–342.
[7] R.E. Henry, H.K. Fauske, Two-phase critical flow at low qualities, part 1: experimental, Nucl. Sci. Eng. 41 (1970) 79–91.
[8] R.E. Henry, H.K. Fauske, Two-phase critical flow at low qualities, part II: analysis, Nucl. Sci. Eng. 41 (1970) 92–98.
[9] S. Rahman, N. Ghadiali, D. Paul, G. Wilkowski, Probabilistic Pipe Fracture Evaluations for Leak-rate-detection Applications, USNRC Report NUREG/CR-6004, U.S. Nuclear Regulatory Commission, Washington, DC, 1995.
[10] PRO-LOCA-GUI/PRO-LOCA, User's Guide (Version 3.5.32), Battelle, Columbus, OH, 2009.
[11] J.H. Park, Y.K. Cho, S.H. Kim, J.H. Lee, Estimation of leak rate through circumferential cracks in pipes in nuclear power plants, Nucl. Eng. Technol. 47 (2015) 332–339.